Exposure dose effects on the reaction-diffusion process in model extreme ultraviolet photoresists

Kristopher A. Lavery, Bryan D. Vogt, Vivek M. Prabhu,[a] Eric K. Lin, and Wen-Li Wu
Polymers Division, National Institute of Standards and Technology, Gaithersburg, Maryland 20899-8541

Sushil K. Satija
Center for Neutron Research, National Institute of Standards and Technology, Gaithersburg, Maryland 20899-8541

Kwang-Woo Choi[b]
Intel Corporation, Santa Clara, California 95052

(Received 29 June 2006; accepted 2 October 2006; published 30 November 2006)

The effect of exposure dose on the latent image deprotection profile in a model extreme ultraviolet (EUV) photoresist polymer, poly(hydroxystyrene-*co*-d_9-*tert*-butyl acrylate), is measured with neutron reflectometry. As the photoacid concentration is increased by exposure dose, the spatial extent of propagation increases but eventually becomes self-limited by the products of the reaction. A long-range deprotection path occurs with diffusion length between 10 and 100 Å, while an additional subnanometer short-range deprotection length scale proceeds monotonically with dose. These measurements show that the photoacid diffusion length into unexposed regions of a photoresist is limited even in the absence of base quencher additives. These fundamental data can be used to highlight materials effects on photoresist processing and to improve quantitative models for EUV photoresists needed at the sub-32-nm half pitch lithography. © *2006 American Vacuum Society.* [DOI: 10.1116/1.2375086]

I. INTRODUCTION

The need for high-throughput fabrication of sub-32-nm half pitch lithographic features continues to drive next-generation semiconductor technologies. While polymer-based chemically amplified photoresists continue to enable lithographic fabrication,[1] the interplay of exposure dose, photoacid reaction-diffusion, and the development process challenge the fabrication of high quality sub-32-nm half pitch features. In particular, acid diffusion during the postexposure bake (PEB) can contribute to image blur and adversely influence linewidth roughness (LWR).[2–4] The need to control LWR to sub-2-nm (3σ) levels at sub-32-nm critical dimension necessitates a thorough understanding of the reaction-diffusion process occurring at the exposure line edge.[5,6] In addition to the aerial image quality,[7,8] material factors related to photoresist chemistry[9] and photoacid-resist interactions must be understood to identify the origins of LWR in chemically amplified photoresists.[2–4,7,10]

Extreme ultraviolet (EUV) lithography is a leading candidate for sub-45-nm lithography nodes. However, many significant challenges remain before the implementation of EUV lithography into high volume production, including low source power,[11] shot noise, resist film thickness and confinement effects,[12] and photoresist resolution issues.[13] From a resist standpoint, the polymer platform must accommodate increased (as high as 40% by mass) photoacid generator (PAG) loadings[14] to compensate for reduced exposure doses (below 10 mJ/cm^2). Resist film thickness will be reduced to meet feature aspect ratio and film transparency requirements[12] at the expense of etch resistance. Lastly, bases[15,16] are added to formulations to reduce image blur, which simultaneously reduces photoresist sensitivity. An improved framework of how these interdependent factors affect the reaction-diffusion process[17–21] is necessary to address imaging quality for EUV lithography.

In this article, we quantify the effect of exposure dose on the reaction-diffusion process in a model EUV photoresist using neutron reflectometry. A polymer-polymer bilayer geometry is used to mimic an ideal step-exposure line edge as described previously by Lin *et al.*[19] and Stewart *et al.*,[22] where the initial photoacid distribution is a step profile that broadens upon undergoing PEB. This sample configuration is prepared by loading the bottom polymer layer with PAG molecules and having the top layer be a resist copolymer with deuterium-labeled protecting groups.[23] After exposure and postexposure bake, the latent image reaction front was directly measured with subnanometer resolution by neutron reflectometry. The shape of the reaction front at a constant PEB time and temperature does not follow an ideal Fickian diffusion form and is dependent upon the exposure dose. The profile shape and the deprotection chemistry are discussed to highlight the important role of the photoacid concentration on the form of the latent image in a model photoresist.

II. EXPERIMENTAL METHODS

A. Materials

The resist copolymer, poly(hydroxystyrene-*co*-d_9-*tert*-butyl acrylate) [P(HOSt-*co*-*t*-BA)], was characterized

[a]Author to whom correspondence should be addressed; electronic mail: vprabhu@nist.gov
[b]Electronic mail: kwang-woo.choi@intel.com

by number average relative molecular mass ($M_{r,n}$) $=11\,700$ g mol^{-1}, polydispersity ($M_{r,w}/M_{r,n}$)$=1.75$, and 50/50 comonomer composition by mole (DuPont Electronic Materials). The polymer was synthesized using deuterium-labeled *tert*-butyl acrylate, whereby the nine hydrogens of the *t*-BA protecting group are replaced with deuterium to provide neutron contrast, as shown previously.[24] The acid feeder contains poly(hydroxyladamantylmethacrylate) (PHAdMA) ($M_{r,n}=10\,500$ g mol^{-1}, $M_{r,w}/M_{r,n}=1.12$, DuPont Electronic Materials) and triphenylsulfonium perfluorobutanesulfonate (TPS-PFBS) (Sigma-Aldrich) as the ionic photoacid generator. PHAdMA/TPS-PFBS (6% PAG by mass of solids) solutions were prepared in *n*-butanol with a 2% mass fraction PHAdMA concentration. This solution was spin coated onto clean silicon wafers (76 mm diameter, 700 μm thick, Virginia Semiconductor, Inc.) followed by a postapply bake (PAB) for 1 min at 130 °C. The resist copolymer, P(HOSt-*co*-*t*-BA), was spin coated from a 2% by mass solution in propylene glycol methyl ether acetate (PGMEA) on top of the acid feeder layer, followed by an additional PAB for 1 min at 130 °C. The layer thicknesses were approximately 65 nm for the resist layer and 40 nm for the acid feeder layer. It was ensured that PGMEA is a nonsolvent for the PHAdMA layer and did not swell the polymer. Since PGMEA does not swell PHAdMA, we assume no PAG was leached into the top layer. Bilayer samples were then exposed using 248 nm arc lamp broadband radiation (Oriel Instruments) to achieve doses ranging from 0 to 20 mJ/cm^2. Postexposure bake was carried out at 90 or 130 °C for 30 s.

B. Neutron reflectometry

The buried interface between the acid feeder and resist copolymer layers was measured using neutron reflectometry. These measurements were completed at the NIST Center for Neutron Research on the NG-7 cold neutron reflectometer. The absolute neutron reflectivity was observed at the specular condition, where the angles (θ) of incidence and reflection are equal. The neutron wavelength (λ) used was 4.768 Å with a wavelength divergence ($\Delta\lambda/\lambda$) of 0.025. Data were taken over a Q_z range of 0.006–0.120 Å^{-1}, where $Q_z=4\pi\lambda^{-1}\sin(\theta)$. The specular reflectivity is sensitive to scattering length density variations normal to the plane of the film. Deuterium-labeled *tert*-butyl protecting groups provide enhanced scattering length density contrast between the protected and deprotected forms of the copolymer. This methodology provides subnanometer resolution of the reaction front propagation. Model reflectivity curves were calculated from trial scattering length density profiles using the methods developed by Parratt.[25] The model was then fitted to the experimental data using a Levenberg-Marquardt nonlinear least squares fitting routine with the relevant trial scattering length density and thickness as parameters.[26] Uncertainties were calculated as an estimated standard deviation from the mean. Where the standard deviation limits are smaller than the plot symbols, the brackets were left off for clarity.

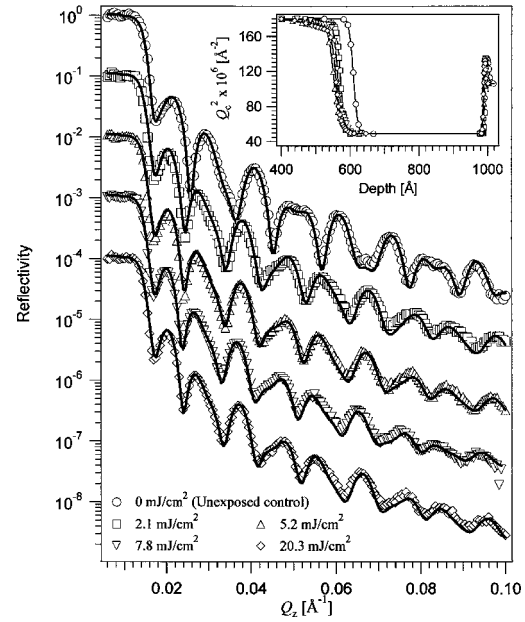

FIG. 1. Reflectivity profiles for polymer-polymer bilayers exposed to 248 nm broadband radiation for the exposure doses listed. PEB was carried out at 90 °C for 30 s. (Inset) Q_c^2 as a function of depth for the doses indicated. Reflectivities are offset for clarity.

C. Spectroscopy

The average deprotection level in the film was quantified by Fourier transform infrared spectroscopy (FTIR). These measurements were performed in transmission using a Nicolet NEXUS 670 spectrometer and a MCT/A detector. The spectra were averaged over 128 scans using a resolution of 8 cm^{-1} to improve the signal-to-noise ratio. The silicon wafers were doubled-side polished, ⟨100⟩ orientation, and *n*-type phosphorous doped with a low resistivity of 1–50 Ω cm to minimize the substrate absorption.

III. RESULTS AND DISCUSSION

The diffusion of photoacid across the model line edge during PEB induces local deprotection of the resist copolymer near the initially sharp polymer-polymer interface. The change in this interfacial structure is measured using neutron reflectometry. Figure 1 shows reflectivity curves for model bilayers after PEB at 90 °C for a series of exposure doses with the absolute reflected intensity plotted versus Q_z. The topmost data set in Fig. 1 corresponds to the unexposed samples, while data corresponding to increasing exposure doses are vertically offset for clarity. The measured reflectivity changes due to the deprotection reaction and the subsequent loss of volatile deuterated deprotection products. The sensitivity of the neutron reflectivity to changes in film interfacial structure is seen in Fig. 1; a shift in the locations of the Kiessig fringes between the exposed and unexposed samples corresponds to decreases in film thickness during PEB. As dose increases from 0 to 7.8 mJ/cm^2, the fringe spacing increases slightly, indicating a decrease in film thickness attributed to the volatile deprotection products. Another important

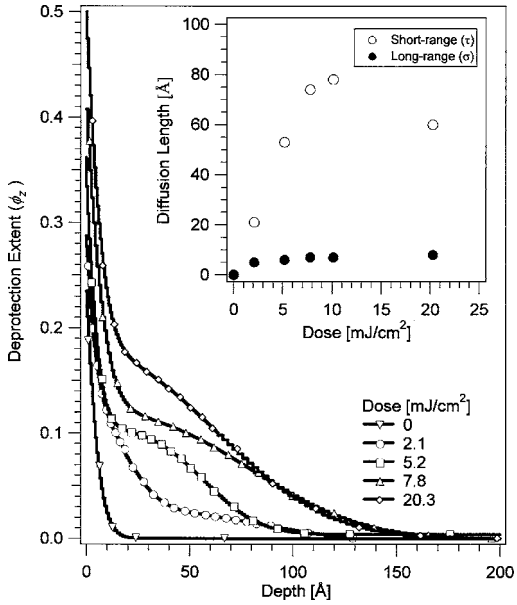

FIG. 2. Deprotection profiles determined from fits to neutron reflectivity data for polymer-polymer bilayer samples exposed to 248 nm broadband radiation for the exposure doses listed. PEB was carried out at 90 °C for 30 s. (Inset) Diffusion lengths for long-range (σ) and short-range (τ) diffusion fronts as a function of exposure dose at 248 nm.

observation is the decrease in the Kiessig fringe persistence with increasing dose. This feature is indicative of a broadening of the buried interface between resist copolymer and the acid feeder layer. These two effects are quantified by modeling the reflectivity data as a polymer-polymer bilayer on top of a silicon oxide/silicon substrate. Model Q_c^2 profiles are shown in the inset to Fig. 1. The accuracy of the fits was improved using deprotection levels obtained from transmission FTIR measurements. The deprotection level obtained by integrating the reaction front deprotection extent through the depth of the film was consistent with the total deprotection level obtained from FTIR.

Using the Q_c^2 profiles obtained from the reflectivity fits, the extent of deprotection $[\phi(z)]$ profile was calculated using the relation

$$\phi(z) = \frac{Q_{c,\text{deprotected}}^2 - Q_c^2}{Q_{c,\text{deprotected}}^2 - Q_{c,\text{protected}}^2}, \tag{1}$$

where the values $Q_{c,\text{deprotected}}^2$ and $Q_{c,\text{protected}}^2$ were independently determined using single layer samples of the resist copolymer and its fully deprotected analog, poly(acrylic acid-*co*-hydroxystyrene). These profiles are shown in Fig. 2 on a plot of $\phi(z)$ versus distance from the interface. A deprotection level of approximately 0.20 is required before the resist copolymer becomes soluble 0.26*N* tetramethylammonium hydroxide developer. The unexposed film has a sharp interface between the copolymer and acid feeder layer with a width less than 2 nm. For an exposure dose of 2.1 mJ/cm^2, the interface broadened appreciably after PEB. This broadening is due to deprotection of the d-*t*-BA in the copolymer and loss of deuterated products. With increasing dose, the width of the interface broadens to a width of 8 nm at a dose of 7.8 mJ/cm^2. The concentration of photogenerated acid, [H+], at this exposure dose can be calculated using the equation

$$[H+] = [\text{PAG}]_0[1 - \exp(-CE)], \tag{2}$$

where $[\text{PAG}]_0$ is the initial photoacid generator concentration, E is the exposure dose, and C is the Dill parameter for PAG in a given polymer.[27] The methodology for estimating the Dill parameter is described elsewhere.[28] The concentration of photogenerated acid at 7.8 mJ/cm^2 is approximately 7.1×10^{-6} mol/ml using a Dill parameter of 0.028 cm^2/mJ for TPS-PFBS within the PHAdMA acid feeder layer. At higher doses, however, the interfacial width does not change significantly but the overall deprotection level in the film increases slightly.

From the best fits to the neutron reflectivity data shown in Fig. 2, the reaction-diffusion front is comprised of two characteristic length scales: σ, for the width of the long-range front, and τ, for the decay length of the short-range front. The short-ranged deprotection length scale becomes more apparent with increasing dose and leads to high levels of deprotection only at the interface between the acid feeder layer and the copolymer. The long-ranged deprotection length comprises a larger fraction of the overall reaction front. The inset to Fig. 2 shows the exposure dose dependence of these two length scales. The short length scale could potentially result from some initial segregation of acid molecules into the protected polymer layer at the interface during sample preparation. Preliminary measurements for photoacid segregation at the interface with x-ray photoelectron spectroscopy are inconclusive. However, bilayer studies of 193 nm (Ref. 29) and 248 nm (Ref. 19) model homopolymer photoresists have not shown this short-range front. Thus, we anticipate that the two different length scales observed are due to the reaction-diffusion process in the copolymer photoresist.

The shape of the measured reaction-diffusion front with varying dose can result from the effect of the changing photoresist composition with increasing extents of reaction. The effect of deprotection extent on the reaction-diffusion rate of PFBS in photoresist polymers was considered by Houle *et al.*[18] They determined the Arrhenius parameters for the diffusion coefficient of PFBS in a homopolymer, poly(*t*-butoxycarbonyloxystyrene) (PBOCSt), and its deprotected form, poly(hydroxystyrene) (PHOSt). A two-order-of-magnitude decrease in the best-fit diffusion coefficient was found between the protected resist (1×10^{-14} cm^2/s at 85 °C) and the polar deprotected form (4×10^{-16} cm^2/s at 85 °C). We compare our results to these by converting the diffusion lengths into one-dimensional reaction-diffusion coefficients using the following expression: $\langle x\rangle = 2(Dt/\pi)^{1/2}$, where $\langle x\rangle$ is the diffusion length, t is the reaction-diffusion time, and D is the diffusion coefficient. In Fig. 3, the diffusion coefficient for the reaction-diffusion process in this model EUV photoresist copolymer is on the same order of magnitude as that predicted in the PBOCSt system. The calculated diffusion rate for the short-range front is on the same

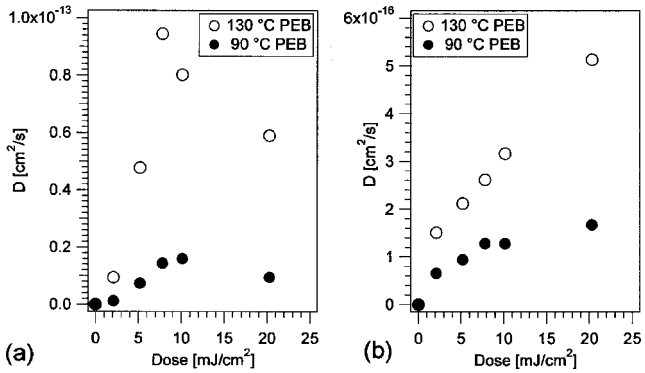

FIG. 3. Diffusion coefficients for the reaction-diffusion fronts, both long-range (a) and short range (b), as a function of exposure dose at 248 nm.

order of magnitude as that for the polar PHOSt. At the interface, we expect a high photoacid concentration, leading to high extents of deprotection (in excess of 35% for the 50% by mole protected copolymer) during PEB that can hinder long-range diffusion of the photoacid. Simultaneously, a long-ranged diffusion front proceeds from the interface into regions of the resist with lower levels of deprotection. The reaction-diffusion coefficient is similar in magnitude to the protected PBOCSt resist because these photoacid molecules experience a resist polarity similar to that of the protected PBOCSt homopolymer. Increasing the photoacid concentration at larger exposure doses results in an increased spatial extent of reaction. This is primarily due to a deprotection reaction rate dependence on the photoacid concentration, resulting in an increase in the reaction-diffusion coefficient D. At higher doses, the increase in resist polarity leads to a slowing of this trend, which can be attributed to hindered photoacid diffusion in a highly polar medium. The ability to control diffusion on the length scales discussed in this work may be critical to patterning chemically amplified photoresists well into sub-32-nm half pitch feature regimes. Means of controlling the long-range diffusion component, either through increasingly polar deprotected resist chemistries or through the use of additives, such as photodegradable base, will be crucial to this effort.

IV. CONCLUSIONS

The spatial extent of the acid catalyzed deprotection front exhibits an exposure dose dependence in a model EUV photoresist polymer. This latent image measured by neutron reflectivity shows the propagation of two different length scales: the slow front results in high deprotection near the ideal exposure interface, while a fast front propagates 10–100 Å into the resist, depending on the exposure dose while maintaining a fixed PEB time and temperature. Since the diffusion lengths depend on the relative amount of photoacid, acid reaction-diffusion models should incorporate the evolving increase in polarity as the reaction proceeds and its influence on acid transport from the exposure line edge.

ACKNOWLEDGMENTS

This work was supported by Intel under CRADA 1893 and the NIST Office of Microelectronics Programs. The authors would like to acknowledge George Thompson, Michael Leeson, Heidi Cao, Hai Deng, Melissa Shell, and Christof Krautschik at Intel Corporation for their support and helpful insights. In addition they would like to thank Jim Sounik and Michael Sheehan at DuPont Electronic Polymers for providing the deuterated copolymers used for these experiments.

[1]H. Ito, Adv. Polym. Sci. **172**, 37 (2005).
[2]J. H. Kim, Y. H. Kim, S. M. Chon, T. Nagai, M. Noda, Y. Yamaguchi, Y. Makita, and H. Nemoto, J. Photopolym. Sci. Technol. **17**, 379 (2004).
[3]G. M. Schmid, M. D. Stewart, V. K. Singh, and C. G. Willson, J. Vac. Sci. Technol. B **20**, 185 (2002).
[4]M. D. Stewart, H. V. Tran, G. M. Schmid, T. B. Stachowiak, D. J. Becker, and C. G. Willson, J. Vac. Sci. Technol. B **20**, 2946 (2002).
[5]R. L. Jones *et al.*, *ACS Symposium Series: Polymers for Microelectronics and Nanoelectronics*, 874 ed. (American Chemical Society, Washington, DC, 2004), p. 86.
[6]J. Nakamura, H. Ban, and A. Tanaka, Jpn. J. Appl. Phys., Part 1 **31**, 4294 (1992).
[7]A. Pawloski, A. Acheta, I. Lalovic, B. La Fontaine, and H. Levinson, Proc. SPIE **5376**, 414 (2004).
[8]S. V. Postnikov *et al.*, J. Vac. Sci. Technol. B **17**, 3335 (1999).
[9]G. Wallraff, J. Hutchinson, W. D. Hinsberg, F. A. Houle, P. Seidel, R. Johnson, and W. Oldham, J. Vac. Sci. Technol. B **12**, 3857 (1994).
[10]W. Hinsberg, F. A. Houle, J. Hoffnagle, M. Sanchez, G. Wallraff, M. Morrison, and S. Frank, J. Vac. Sci. Technol. B **16**, 3689 (1998).
[11]V. Banine and R. Moors, Proc. SPIE **4343**, 203 (2001).
[12]D. L. Goldfarb, M. Angelopoulos, E. K. Lin, R. L. Jones, C. L. Soles, J. L. Lenhart, and W. L. Wu, J. Vac. Sci. Technol. B **19**, 2699 (2001).
[13]R. L. Brainard, J. Cobb, and C. A. Cutler, J. Photopolym. Sci. Technol. **16**, 401 (2003).
[14]A. R. Pawloski and P. F. Nealey, J. Vac. Sci. Technol. B **20**, 2413 (2002).
[15]F. A. Houle, W. D. Hinsberg, and M. I. Sanchez, J. Vac. Sci. Technol. B **22**, 747 (2004).
[16]S. Nagahara *et al.*, Proc. SPIE **5753** (2005).
[17]W. D. Hinsberg, F. A. Houle, M. I. Sanchez, and G. M. Wallraff, IBM J. Res. Dev. **45**, 667 (2001).
[18]F. A. Houle, W. D. Hinsberg, M. Morrison, M. I. Sanchez, G. Wallraff, C. Larson, and J. Hoffnagle, J. Vac. Sci. Technol. B **18**, 1874 (2000).
[19]E. K. Lin *et al.*, Science **297**, 372 (2002).
[20]L. Schlegel, T. Ueno, N. Hayashi, and T. Iwayanagi, J. Vac. Sci. Technol. B **9**, 278 (1991).
[21]M. Zuniga, G. M. Wallraff, and A. R. Neureuther, Proc. SPIE **2438**, 113 (1995).
[22]M. D. Stewart, G. M. Schmid, D. L. Goldfarb, M. Angelopoulos, and C. G. Willson, Proc. SPIE **5039**, 415 (2003).
[23]G. Schmid, M. Stewart, W. Wang, B. Vogt, V. Prabhu, E. Lin, and C. Willson, Proc. SPIE **5376**, 333 (2004).
[24]K. A. Lavery *et al.*, Proc. SPIE **6153**, 615313 (2006).
[25]L. G. Parratt, Phys. Rev. **95**, 359 (1954).
[26]W. Press, *Numerical Recipes: The Art of Scientific Computing* (Cambridge University Press, Cambridge, 1986).
[27]F. H. Dill, W. P. Hornberger, P. S. Hauge, and J. M. Shaw, IEEE Trans. Electron Devices **ED22**, 445 (1975).
[28]S. H. Kang, V. M. Prabhu, B. D. Vogt, E. K. Lin, W.-L. Wu, and K. Turnquest, Polymer **47**, 6293 (2006).
[29]B. Vogt, S. Kang, V. M. Prabhu, A. Rao, E. K. Lin, S. K. Satija, K. Turnquest, and W. L. Wu, Proc. SPIE **6153**, 398 (2006).